The Journal of Immunology

RESEARCH ARTICLE | MARCH 01 2015

Retinoic Acid Imprints a Mucosal-like Phenotype on Dendritic Cells with an Increased Ability To Fuel HIV-1 Infection

Natalia Guerra-Pérez; ... et. al

J Immunol (2015) 194 (5): 2415–2423.
https://doi.org/10.4049/jimmunol.1402623

Retinoic Acid Imprints a Mucosal-like Phenotype on Dendritic Cells with an Increased Ability To Fuel HIV-1 Infection

Natalia Guerra-Pérez,* Ines Frank,* Filippo Veglia,* Meropi Aravantinou,* Diana Goode,* James L. Blanchard,† Agegnehu Gettie,‡ Melissa Robbiani,*,[1] and Elena Martinelli*,[1]

The tissue microenvironment shapes the characteristics and functions of dendritic cells (DCs), which are important players in HIV infection and dissemination. Notably, DCs in the gut have the daunting task of orchestrating the balance between immune response and tolerance. They produce retinoic acid (RA), which imprints a gut-homing phenotype and influences surrounding DCs. To investigate how the gut microenvironment impacts the ability of DCs to drive HIV infection, we conditioned human immature monocyte-derived DCs (moDCs) with RA (RA-DCs), before pulsing them with HIV and mixing them with autologous T cells. RA-DCs showed a semimature, mucosal-like phenotype and released higher amounts of TGF-β1 and CCL2. Using flow cytometry, Western blot, and microscopy, we determined that moDCs express the cell adhesion molecule mucosal vascular addressin cell adhesion molecule-1 (MAdCAM-1) and that RA increases its expression. MAdCAM-1 was also detected on a small population of DCs in rhesus macaque (*Macaca mulata*) mesenteric lymph node. RA-DCs formed more DC–T cell conjugates and promoted significantly higher HIV replication in DC–T cell mixtures compared with moDCs. This correlated with the increase in MAdCAM-1 expression. Blocking MAdCAM-1 partially inhibited the enhanced HIV replication. In summary, RA influences DC phenotype, increasing their ability to exacerbate HIV infection. We describe a previously unknown mechanism that may contribute to rapid HIV spread in the gut, a major site of HIV replication after mucosal exposure. ***The Journal of Immunology*****, 2015, 194: 2415–2423.**

Since the 1990s, it is known that dendritic cells (DCs) mediate HIV *trans*-infection of $CD4^+$ T cells (1, 2). This results in a burst of virus replication that is much greater than that resulting from direct, *cis* infection of either DCs or T cells, or *trans* infection between T cells (1, 3). Such DC-to-T cell *trans* infection involves a complex sequence of steps, as follows: attachment, entry, and replication patterns that may have similarities among APCs, but also differences in the receptors involved, intracellular trafficking, and productive and nonproductive replication pathways (4–6). Importantly, because DCs reside in submucosal tissues, they are thought to be among the first cells that encounter HIV following sexual transmission (7, 8). However, DC phenotype and function are determined by the microenvironment, and their ability to fuel HIV infection may change according to the type of DC and their anatomical location (9). How the mucosal environment shapes a DC's ability to transfer the virus to T cells and their susceptibility to HIV has never been addressed.

The gut and the gut inductive sites, mesenteric lymph nodes (MLNs) and Peyer's patches (PPs), are major sites of early HIV and SIV replication and amplification, resulting in profound and rapid $CD4^+$ T cell loss (10, 11). $CD4^+$ T cells in the intestinal tract are infected 10-fold more frequently than those in blood (12, 13). Moreover, the depth of $CD4^+$ T cell depletion in the gut mucosa is associated with progression to AIDS (14, 15). The underlying mechanisms that render the gut and the gut-associated lymphoid tissue (GALT) especially receptive to HIV replication are not fully understood.

Due to the continuous exposure to dietary Ags and commensal microbes, the gut represents a unique immunological environment, requiring a balance between prompt, effective responses to pathogens and tolerance to innocuous Ags. Appropriate mucosal immune responses depend on specialized DCs (16), and the gut microenvironment has a key role in imprinting on DCs the unique ability to mediate both T cell priming/activation and tolerance (17). One of the major players in the maintenance of the balance between immunity and tolerogenicity is retinoic acid (RA). Depending on the presence of other soluble factors in the gut microenvironment, including TGF-β1, IL-6, and IL-10, RA is able to sway the T cell responses toward a T regulatory or a Th17 phenotype (18–20). RA released by intestinal epithelial cells and lamina propria (LP) stromal cells primes LP gut DCs to become $CD103^+$ mucosal DCs (21–24). A distinctive characteristic of $CD103^+$ mucosal DCs,

*Center for Biomedical Research, Population Council, New York, NY 10065; †Tulane National Primate Research Center, Tulane University, Covington, LA 70433; and ‡Aaron Diamond AIDS Research Center, The Rockefeller University, New York, NY 10016

[1]M.R. and E.M. are equal senior authors.

Received for publication October 15, 2014. Accepted for publication January 3, 2015.

This work was supported by National Institutes of Health Base Grants R37 AI040877-15 and R01 AI098456-01 and United States Agency for International Development Cooperative Agreement GPO-A-00-04-00019-00. Additional support was provided by Tulane National Primate Research Center Base Grant OD011104. N.G.-P. is an F.M. Kirby Foundation fellow, and M.R. is a 2002 Elizabeth Glaser scientist.

Address correspondence and reprint requests to Dr. Elena Martinelli, Center for Biomedical Research, Population Council, 1188 York Avenue, New York, NY 10065. E-mail address: emartinelli@popcouncil.org

The online version of this article contains supplemental material.

Abbreviations used in this article: DC, dendritic cell; GALT, gut-associated lymphoid tissue; HEV, high endothelial venule; iTreg, induced regulatory T cell; LN, lymph node; LP, lamina propria; MAdCAM-1, mucosal vascular addressin cell adhesion molecule-1; MLN, mesenteric lymph node; moDC, monocyte-derived DC; PP, Peyer's patch; RA, retinoic acid; RAR, RA receptor; RT, room temperature; TNPRC, Tulane National Primate Research Center.

not possessed by DCs from other anatomical sites, is the ability to metabolize vitamin A into RA (25). Through their ability to produce RA, mucosal DCs modulate T and B cell phenotype and induce the expression of integrin $\alpha_4\beta_7$, the gut-homing receptor (26). Notably, $\alpha_4\beta_7^{high}$ $CD4^+$ T cells are highly susceptible to HIV infection and are preferentially depleted during the early, acute stages after mucosal transmission (27, 28). Recently, we showed that their frequency in the rectal mucosa is associated with susceptibility to rectal SIV infection (29) and in vivo blocking of $\alpha_4\beta_7$ reduces susceptibility to vaginal SIV transmission (30).

The $\alpha_4\beta_7$ ligand, mucosal vascular addressin cell adhesion molecule-1 (MAdCAM-1), is predominantly expressed on high endothelial venules (HEV) of the GALT and on venules at chronically inflamed mucosal sites (31). However, MAdCAM-1 has the potential to be expressed outside the endothelial cell lineage, for example, by fibroblasts, melanoma cells, and mesenchymal follicular DCs (32). MAdCAM-1 expression by DCs of monocyte lineage has never been reported.

In this work, we describe how the gut microenvironment can shape the ability of DCs to promote and respond to HIV infection. We define the mucosal-like phenotype of RA-conditioned human monocyte-derived DCs (RA-DCs), and we reveal their increased capacity to form DC–T cell conjugates and release TGF-β1 and CCL2 (MCP-1). Notably, to our knowledge, we report for the first time MAdCAM-1 detection on DCs and its upregulation by RA. Finally, we found that RA treatment of DCs enhances their ability to drive HIV replication in the DC–T cell milieu compared with immature monocyte-derived DCs (moDCs), and this is partially mediated by MAdCAM-1 interaction with $\alpha_4\beta_7$ on the $CD4^+$ T cells.

Materials and Methods

Ethics statement

Tissues from 15 healthy SIV-uninfected adult female Indian rhesus macaques (*Macaca mulatta*) being used for a separate study were used to detect MAdCAM-1 in DCs in vivo. The animals were housed in compliance with the regulations under the Animal Welfare Act, the *Guide for the Care and Use of Laboratory Animals*, at Tulane National Primate Research Center (TNPRC, Covington, LA). Animals were socially housed indoors in climate-controlled conditions with a 12/12-light/dark cycle. Animals were monitored continuously by veterinarians to ensure their welfare and fed commercially prepared monkey chow twice daily. Water was available at all times. The TNPRC environmental enrichment program is reviewed and approved by the Institutional Animal Care and Use Committee semiannually. All of the animals were euthanized using methods consistent with recommendations of the American Veterinary Medical Association Panel on Euthanasia and per the recommendations of the Institutional Animal Care and Use Committee. Specifically, the animals were anesthetized with tiletamine/zolazepam (8 mg/kg i.m.) and given buprenorphine (0.01 mg/kg i.m.), followed by an overdose of pentobarbital sodium. Death was confirmed by auscultation of the heart and pupillary dilation. All studies were approved by the Animal Care and Use Committee of the TNPRC (OLAW assurance A4499-01) and in compliance with animal care procedures. TNPRC is accredited by the Association for Assessment and Accreditation of Laboratory Animal Care (AAALAC 000594).

Cell isolation and culture

Macaque iliac lymph nodes (LNs) and MLNs were obtained at necropsy, cut in small pieces, and passed through a 40-μm cell strainer. PBMCs were isolated from macaque blood and human leukopacks (New York Blood Center) using Ficoll-Hypaque density gradient centrifugation (Amersham Pharmacia Biotech GE Healthcare, Little Chalfont, U.K.). Human $CD14^+$ monocytes were isolated using the CD14 magnetic cell-sorting system (Miltenyi Biotec, Auburn, CA); moDCs were generated by culturing monocytes in 100 U/ml IL-4 (Life Technologies, Life Technologies); and 1000 U/ml GM-CSF (Biosource, Life Technologies) was added every 2 d. Cells were cultured for 6 d at 10^6 cells/ml in 6-well plates in R1 (RPMI 1640, 1% human plasma + 2 mM L-glutamine, 10 mM HEPES, Pen/Strep). On day 4, cells were also treated with different concentrations of RA (Sigma-Aldrich, St. Louis, MO; RA-DCs) or mock treated (DMSO, Sigma-Aldrich; moDCs). On day 6, their phenotype was analyzed by multicolor flow cytometry. Autologous $CD14^-$ cells were kept in culture in R10 (RPMI 1640, 10% FBS + L-glutamine, HEPES, Pen/Strep) with 1 U/ml IL-2 (National Cancer Institute Preclinical Repository). On day 5, $CD4^+$ T cells were isolated from $CD14^-$ cell cultures using the CD4 T cell isolation kit (Miltenyi Biotec). $CD4^+$ T cells were cultured for 1 d in R5 (RPMI 1640, 5% human serum + 2 mM L-glutamine, 10 mM HEPES, Pen/Strep) with 1 U/ml IL-2.

HIV-loaded DCs and DC–T cell cultures

HIV-BaL was provided by the AIDS and Cancer Virus Program (SAIC Frederick, National Cancer Institute, Frederick, MD). moDCs and RA-DCs were pulsed with HIV (8×10^4 tissue culture-infective dose $50/10^6$ DCs) for 2 h at 37°C in a 15-ml conical tube at a concentration of 10^7 DCs/ml. Cells were washed three times before recounting them and mixing them with T cells in R5 (1 U/ml IL-2). A total of 10^5 DCs was added to 3×10^5 $CD4^+$ T cells (per well of a 96-flat-well plate) in triplicates in the absence or presence of 500 nM αRA receptor (RAR; LE540, Wako Chemical USA, Richmond, VA; Ro 41-5253, Enzo Life Sciences, Farmingdale, NY). For the MAdCAM-1 blocking experiments, 10^5 HIV-loaded moDCs and RA-DCs were incubated with 5 μg/ml anti-human MAdCAM-1 mAb (clone 314G8; Bio-Rad AbD Serotec, Raleigh, NC) or 5 μg/ml IgG1 control (Bio-Rad AbD Serotec) in a 96-flat-well plate for 20 min at 4°C before the addition of 3×10^5 $CD4^+$ T cells (1.25 μg/ml final concentration). No additional anti–MAdCAM-1 was added during the culture. After 9 d, the cells were harvested and HIV–quantitative PCR was performed on cell lysates, as previously described (33). For the analysis of HIV capture by DCs, HIV-loaded moDCs and RA-DCs were permeabilized and stained, immediately after the HIV pulse, with FITC anti-p24 mAb (Beckman Coulter, Brea, CA). For the infection of moDCs and RA-DCs, HIV-loaded DCs were seeded in a 96-well flat-bottom plate (3×10^5 DCs/well) in the absence or presence of αRAR. Samples were set up in triplicate in R1 (IL-4/GM-CSF supplemented). Six days later, DCs were harvested and HIV–quantitative PCR was performed on the cell lysates. For the analysis of moDC–T cell and RA-DC–T cell conjugates and T cell phenotype, 10^5 DCs, without HIV, were seeded in triplicate in R5 (1 U/ml IL-2) in a 96-well flat-bottom plate with 3×10^5 cells $CD4^+$ T cells in the absence or presence of αRAR and in the absence or presence of 10 μg/ml anti–MAdCAM-1 mAb (314G8; AbD Serotec) or of an anti-CD54 (AbD Serotec) or both. Five days later, DC–T cell cultures were harvested, and the cells were stained for flow cytometry.

Flow cytometry

Cells were incubated with the Live/Dead Aqua dye (Molecular Probes, Life Technologies, Carlsbad, CA) before surface staining. mAbs included in the human DC panel were as follows: anti–CD11c-AF700 (eBioscience, San Diego, CA); anti–CD1c-allophycocyanin (Miltenyi Biotec); anti–β7-allophycocyanin (BioLegend, San Diego, CA); anti–CD29-allophycocyanin and anti–CD103-allophycocyanin (eBioscience); anti–CD4-APCH7, anti–CD80-APCH7, and anti–CD103-FITC (eBioscience); anti–CD206-FITC, anti–CD209-FITC, and anti–CD11b-PCPCy5.5 (BioLegend); anti–CXCR4-PCPCy5.5 and anti–MAdCAM-1-PE (AbD Serotec); dimeric anti–$\alpha_4\beta_7$-PE (clone Act1; NHP Reagent Resource, MassBiologics, University of Massachusetts, Boston, MA); anti–CD25-PeCy7 (BioLegend); anti–CD206-PeCy7 (BioLegend); anti–HLA-DR-QDot605 (Invitrogen, Life Technologies); and anti–CD14-V450. The following mAbs, CCR5-PeCy7, CD103-PeCy7, CD141-PeCy7, and CD54-PCPCy5.5, were directly conjugated using the Lightning-Link kits (Innova Biosciences, Cambridge, U.K.). For the T cell phenotype in uninfected DC–T cell cultures, the panel included the following: anti–CD69-AF700, anti–CD45RO-allophycocyanin, anti–CD62L- allophycocyanin, anti–CD4-APCH7, anti–CD45RA-FITC, anti–PD-1-PCP-efluor710 (eBioscience), anti–$\alpha_4\beta_7$-PE, anti–HLA-DR-QDot605, and anti–CD3-V450 (all the mAbs were from BD Biosciences, San Jose, CA, unless otherwise indicated). After surface staining, the cells were fixed and permeabilized with fix/perm buffer and incubated with anti–FOXP3-FITC (eBioscience) for 45 min at room temperature (RT). For macaque cells, the following mAbs were used: CD11c-AF700 (eBioscience), CD14-V450, CD3-V450, CD20-V450, HLA-DR BV605, CD4-APCH7, CD45RA-FITC, CD103-allophycocyanin, and MAdCAM-1-PE. The CCR7-PeCy7 and dimeric $\alpha_4\beta_7$-PeCy7 mAbs were directly conjugated using Lightning-Link labeling kits (Innova Biosciences). For the binding of recombinant $\alpha_4\beta_7$ (R&D Systems, Minneapolis, MN) to moDCs and T cells, biotinylated (E-Z Link biotinylation reagent; Pierce Thermo Scientific, Rockford, IL) $\alpha_4\beta_7$ was incubated with the cells 20 min at 4°C, washed, and detected with PE-Neutravidine (Pierce Thermo Scientific). The buffer was HEPES-buffered saline with 100 mM $CaCl_2$ and 1 mM $MnCl_2$. At least 200,000 events were

acquired using the LSRII (BD Biosciences), and FlowJo-V9 (Tree Star, Ashland, OR) was used to analyze the data.

Western blot

Day 6 moDCs and RA-DCs (2×10^6 cells) were lysed with lysis buffer (NuPAGE LDs; Life Technologies). Total cell lysates were subjected to electrophoresis under manufacturer's conditions (NuPAGE Bis-Tris Mini Gels; Life Technologies) and transferred onto polyvinylidene difluoride membranes (Invitrogen). Membranes were blocked for 2 h with 5% nonfat dry milk in PBS 0.05% Tween 20 (PBS-T) and incubated in 1% dry milk with primary mAbs (anti–MAdCAM-1 clones 17F5, 314G8 [AbD Serotec], and CA2.2 [eBioscience] and anti–β-actin [Abcam, Cambridge, MA]) at a 1:1000 dilution overnight at 4°C. The membranes were washed with PBS-T, incubated with HRP-secondary Abs diluted 1:3000 in 1% PBS-T at RT for 1 h, and washed with PBS-T. The immunoreactive bands were detected by chemiluminescence reagent (Thermo Scientific, Waltham, MA), visualized on SuperRX film (Thermo Scientific), and quantified (after normalization on β-actin) using ImageJ (National Institutes of Health, Bethesda, MD).

Detection of soluble proteins

The concentration of TGF-β1 in the supernatants was measured by ELISA (R&D Systems). Samples were measured with and without the chemical activation step suggested by the manufacturer and analyzed for the presence of cytokines and chemokines using the Cytokine Human 25-Plex Panel kit (Invitrogen), according to the manufacturer's protocol. The kit allows for the measurement of GM-CSF, IL-1β, IL-1RA, IL-6, CXCL8, TNF-α, IFN-γ, IL-2, IL-2R, IL-4, IL-5, IL-10, IFN-α, IL-7, IL-12, IL-13, IL-15, IL-17, CXCL10, CCL2, CXCL9, CCL5, CCL3, and CCL4. The data were detected with the Luminex 200 System and analyzed using xPONENT v3.1 Software (Life Technologies).

Microscopy

Cells were adhered to glass slides coated with Alcian blue (Sigma-Aldrich) and fixed with 3.7% paraformaldehyde 10 min at 4°C. PBS-BSA 1% was used to dilute Abs and rinse the cells between incubation steps. All steps were performed at RT. Nonspecific staining was blocked with 10% sheep serum (Sigma-Aldrich) in PBS for 20 min before being immunostained with an anti–MAdCAM-1 mAb (Bio-Rad AbD Serotec; clone 314G8; 20 μg/ml) or the isotype control (mIgG1; 20 μg/ml) for 30 min. Bound Abs were detected by adding a goat anti-mouse AF488 (2.5 μg/ml) for 30 min. For the detection of MAdCAM-1 on HEV of macaque MLNs, formalin-fixed paraffin-embedded 5-μm slices of tissue were prepared at the TNPRC. Deparaffinization was achieved by incubation three times in xylene for 5 min, three times in 100% EtOH for 2 min, once in 95% EtOH for 2 min, once in 80% EtOH for 2 min, and twice in distilled water for 2 min. For Ag retrieval, slides were incubated 20 min in Diva Decloaker (Biocare Medical, Concord, CA) at 98°C. Tissues were incubated 40 min in blocking buffer (PBS, 0.2% fish skin gelatin, 10% normal goat serum, 1% BSA), washed in washing buffer (PBS, 0.2% fish skin gelatin, 0.1% Triton X-100), and incubated 1 h at RT in the dark with AF568 anti–MAdCAM-1 (clone 314G8; AbD Serotec) or mouse IgG1 negative control diluted 1:100 in blocking buffer. Slides were mounted with ProLong gold with DAPI mounting media (Molecular Probes, Life Technologies). Images were captured on a wide-field fluorescence microscope (motorized Z-drive; Zeiss) equipped with a Hamamatsu Orca ER B/W digital camera and MetaVue Acquisition Software (Molecular Devices, Sunnyvale, CA) using a plan apochromat ×40 or ×100 oil immersion objective. The images were processed with ImageJ software (National Institutes of Health, Bethesda, MD).

Statistics

The different conditions were compared using nonparametric Wilcoxon signed-ranked test. The correlation between the fold increase in mean fluorescence intensities and fold increase in HIV replication was analyzed with linear regression analysis, and the p value of the Spearman rank coefficient analysis was used to determine significance. The analysis was performed using GraphPad Prism 5.03 (GraphPad InStat, San Diego, CA).

Results

RA promotes a semimature mucosal-like phenotype on DCs

To examine how the RA-rich gut microenvironment influences the phenotype and function of DCs, we conditioned human moDCs with RA (RA-DCs), adapting a protocol for the generation of mucosal DCs from murine bone marrow cells (21). After generating immature moDCs by culturing $CD14^+$ monocytes with GM-CSF and IL-4 for 4 d, the cells were cultured for additional 2 d in presence of RA or a mock solution (to generate RA-DCs versus moDCs side by side). Multicolor flow cytometry at day 6 revealed that RA treatment significantly increased the expression of HLA-DR, CD25, CD141, CD11b, and β_7, but reduced expression of CD206, and had limited or no effect on CD80, CD1c, CD209, and $\alpha_4\beta_7$ (relative to moDC controls) (Fig. 1, Supplemental Fig. 1A). Remarkably, the HIV receptors CD4, CCR5, and CXCR4 were all significantly upregulated by RA treatment. Moreover, the expression of CD103, a marker of mucosal DCs (16, 17, 34), and CD54, involved in the formation of DC–T cell synapses (35), was also significantly higher on RA-DCs than on mock-treated moDCs. Initial experiments in which moDCs were treated with different concentrations of RA revealed that treatment with 0.1 μM RA consistently resulted in more significant changes than treatment with the other concentrations of RA tested (Supplemental Fig. 1B). Thus, we decided to explore further the biology of RA-DCs treated with 0.1 μM RA. Addition of RA to moDC cultures at day 3 instead of day 4 did not substantially change its effect on the moDC phenotype (data not shown). We did not test the addition of RA to the $CD14^+$ monocytes at the beginning of the culture, as published in a previous report (36), because that would not mimic the effect of RA on developed immature DCs as it occurs in the gut microenvironment.

We found that RA-DCs released more total TGF-β1 than moDCs (Fig. 2, Supplemental Fig. 2A) in all the samples tested with the exception of one donor (of eight) that had 4 times less TGF-β1 in RA-DCs than moDCs. The donor was excluded from the analysis and the data reported. We measured also the bioactive form of TGF-β1, testing the samples without the chemical activation step required by the assay. The donor with the highest amount of total TGF-β1 had a detectable amount of bioactive TGF-β1 in the supernatant of the RA-DCs (15.3 pg/ml), but none in the moDCs. All of the other RA-DC and moDC samples had no detectable bioactive TGF-β1. Notably, RA-DCs released significantly more CCL2, a Th2 response-inducing factor (37), than control moDCs (Fig. 2, Supplemental Fig. 2A). RA-DCs also released small amounts of the anti-inflammatory cytokine IL-10, compared with almost undetectable amounts produced by moDCs. In line with their semimature phenotype, RA-DCs also released slightly more inflammatory cytokines, as follows: IL-6, CXCL8 (IL-8), IL-12 (IL-12p40/p70), and IFN-α (Fig. 2, Supplemental Fig. 2A). RA-DCs consistently produced more IL-2R than moDCs, but this was not significant ($p = 0.07$).

MAdCAM-1 is detected on moDCs and on DCs in MLNs

MAdCAM-1 is constitutively expressed by HEVs of PPs and MLNs as well as on postcapillary venules of gut LP, but has the potential to be expressed outside the endothelial cell lineage (32). MAdCAM-1 has been detected also on fibroblastic-like cells and follicular DCs (38). Remarkably, using flow cytometry, Western blot, and microscopy, we detected MAdCAM-1 on moDCs (Fig. 3, Supplemental Fig. 1A). Interestingly, MAdCAM-1 was recognized by the 314G8 and CA2.2 clones (Fig. 3, and data not shown), which bind the Ig domain of the protein, but not by the 17F5 clone that binds the mucin domain (Fig. 3B). By microscopy, MAdCAM-1 appears to be similarly distributed in small clusters on the moDC and RA-DC surfaces (Fig. 3C). By flow cytometry we found that surface expression of MAdCAM-1 was higher on RA-DCs than on moDCs, and this was supported by the microscopy. However, the increase in total MAdCAM-1 detected by Western blot was less pronounced. Finally, we also verified binding of PE-conjugated recombinant $\alpha_4\beta_7$ to moDCs. In contrast, binding to T cells was not detected (Supplemental Fig. 2B).

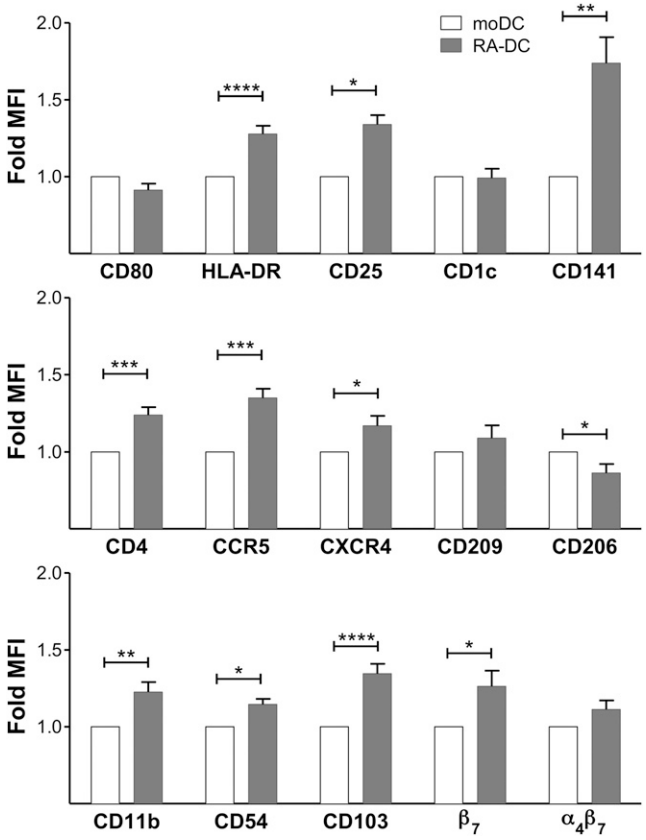

FIGURE 1. RA-DCs show a semimature mucosal-like phenotype. moDCs and RA-DCs were gated on live, single, CD11c$^+$ cells. The fold increase (mean ± SEM, n = 4–41) of the mean fluorescence intensity of each marker on RA-DCs is shown compared with the control moDCs (set as 1) (*$p < 0.05$ is considered significant: **$p < 0.01$, ***$p < 0.001$, ****$p < 0.0001$).

To explore whether MAdCAM-1 can be expressed by DCs in vivo, we tested the binding of the anti–MAdCAM-1 mAb clone 314G8 on DCs from different rhesus macaque tissues. Once confirmed that the 314G8 clone recognizes MAdCAM-1 on the HEV of macaque MLNs (Fig. 4A), we performed multicolor flow cytometry on cells from MLNs, iliac LNs, and blood to search for MAdCAM-1–positive cells with a clear DC phenotype. We detected a small, but distinct population of Lin$^-$ HLA-DR$^+$ DCs that expressed MAdCAM-1 in 15 of 15 MLNs tested (Fig. 4B; range, 0.58–2.98%; mean = 1.1%). In contrast, reactivity to the anti–MAdCAM-1 mAb could barely be detected (above the isotype controls) in iliac DCs (range, 0.00–0.67%; mean = 0.29%) or blood DCs (range, 0.04–0.79%; mean = 0.24%). The majority of MAdCAM-1$^+$ DCs in the MLNs were CD11c^{low}, CD103$^+$, and CCR7$^-$ (Fig. 4C).

RA-DCs form more DC–T cell conjugates and induce a regulatory CD4$^+$ T cell phenotype

To determine the impact that the RA treatment has on the DC's ability to drive phenotypic changes in CD4$^+$ T cells, we cocultured RA-DCs and moDCs with autologous CD4$^+$ T cells for 5 d. Before mixing RA-DCs with the T cells, the DCs were extensively washed to remove exogenous RA. However, RA treatment is known to induce RA-producing capability on DCs (21, 36). Thus, to distinguish the effect of RA-DC–derived RA from the effect of other RA-DC–specific characteristics on the CD4$^+$ T cells, we treated half of the CD4$^+$ T cells with RAR antagonists (RARα and RARβ antagonists Ro 41-5253 and LE540; here together: αRAR) prior to mixing them with the DCs. All of the DC–T cell experiments were performed in presence of αRAR or a mock solution in parallel.

Interestingly, we found a higher frequency of DC–T cell conjugates in the RA-DC–T cell cocultures than in the moDC–T cell mixtures both in the presence and absence of αRAR (Fig. 5A). The frequency of conjugates was not affected by treatment with the αRAR (Supplemental Fig. 2C). Moreover, in agreement with other in vitro models of mucosal DCs (21), we found that the RA-DCs increase the expression of $\alpha_4\beta_7$ on cocultured CD4$^+$ T cells. Specifically, we found a higher frequency of $\alpha_4\beta_7^{high}$ memory CD4$^+$ T cells (Fig. 5B, Supplemental Fig. 3) in RA-DC–T cell mixtures than in the moDC–T cell mixtures. We also observed higher expression of FOXP3, PD1, and CD69, markers of induced regulatory T cells (iTreg) (39, 40) on the CD4$^+$ T cells cocultured with the RA-DCs (Fig. 5B, Supplemental Fig. 3). Notably, these increases occurred also in presence of the αRAR, suggesting they were not exclusively dependent on the RA produced by the RA-DCs as it was reported for T cells cocultured with TLR-ligand–stimulated RA-DCs (21, 36).

RA-DCs promote greater HIV replication than moDCs in DC–T cell mixtures

Considering the impact of RA on the DC phenotype and the effect of the RA-DCs on the T cells, we hypothesized that RA may change the ability of DCs to spread HIV infection. To demonstrate this, we cocultured HIV-loaded RA-DCs and moDCs with autologous CD4$^+$ T cells. Because RA can induce T cell activation and modulate

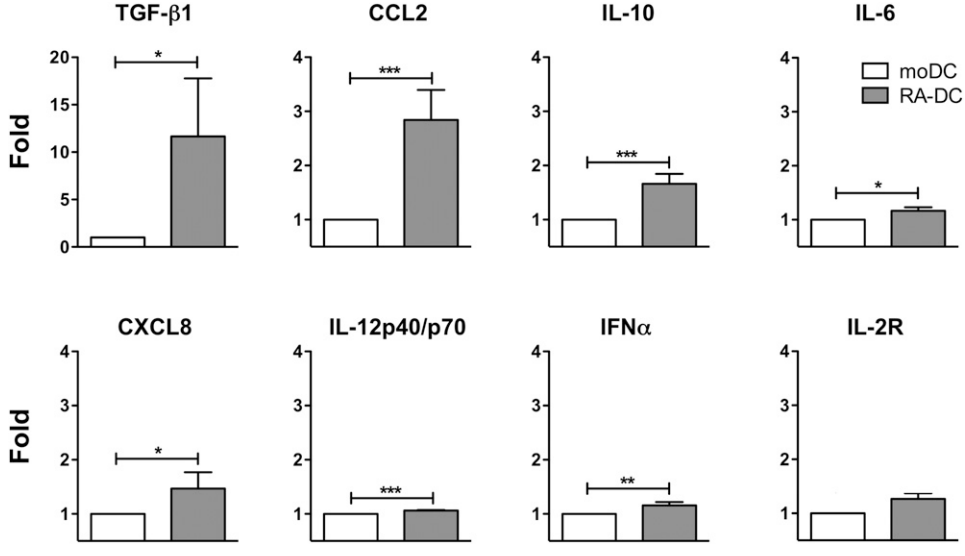

FIGURE 2. RA-DCs release tolerogenic cytokines. The fold increase (mean ± SEM, n = 8) in the concentration of the indicated soluble factors in the supernatants of RA-DCs is shown compared with the control moDCs (set as 1) at day 6 of culture. The data from one donor were excluded for TGF-β1, because this donor had 4-fold less TGF-β1 in RA-DCs than in moDCs. This was in contrast with all other donors showing the opposite trend (*$p < 0.05$, **$p < 0.01$, ***$p < 0.001$).

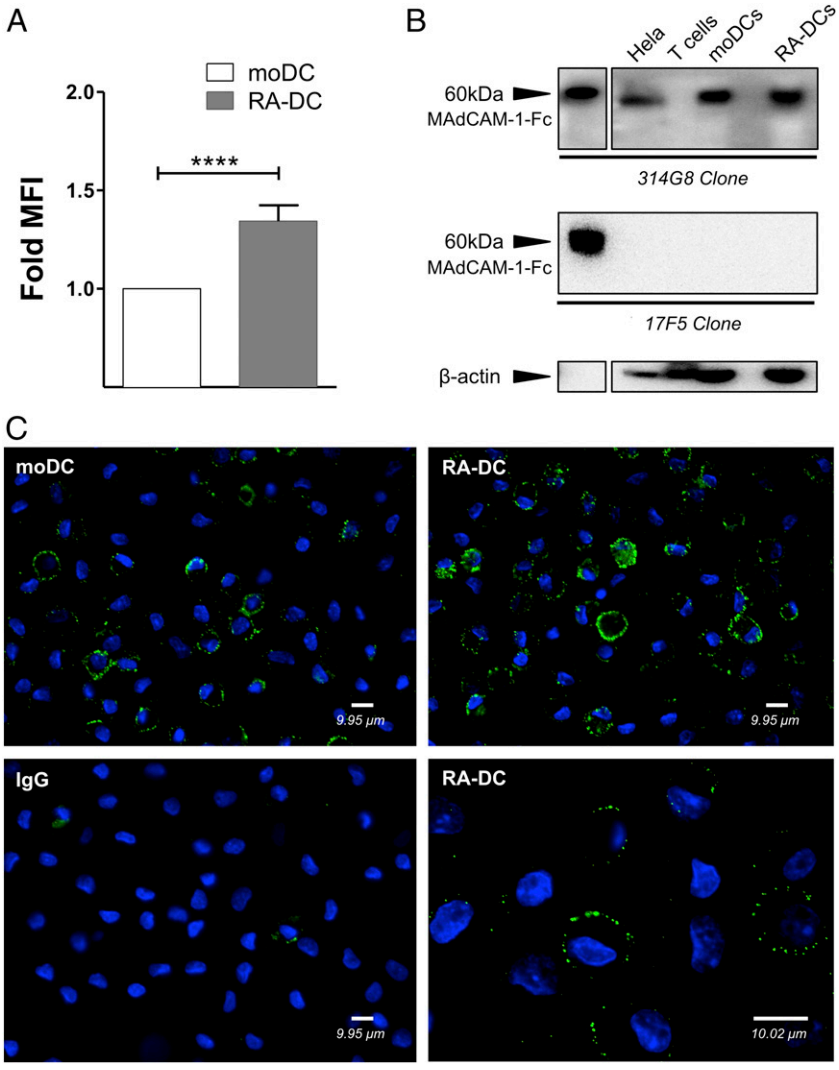

FIGURE 3. MAdCAM-1 is detected on moDCs, and RA treatment increases its expression. (**A**) moDCs and RA-DCs were gated on live, single, $CD11c^+$ cells. The fold increase (mean ± SEM, $n = 39$) of MAdCAM-1 mean fluorescence intensity on RA-DCs is shown compared with the control moDCs (set as 1). $p < 0.05$ is considered significant (****$p < 0.0001$). (**B**) Representative blots of MAdCAM-1 detection in total lysates of moDCs, RA-DCs, $CD4^+$ T cells (negative control), and HeLa cells (cell lysate positive control) with anti–MAdCAM-1 mAbs (clones 314G8 upper membrane and 17F5 middle membrane). Soluble MAdCAM-Fc (MAdCAM-1) was used as positive control. Anti–β-actin mAb was used for normalization (lower membrane). RA-DCs expressed slightly more total MAdCAM-1, 1.18 ± 0.06-fold (mean ± SEM, $n = 7$), when comparing the fold intensity of normalized MAdCAM-1 content in RA-DCs compared with the control moDCs (set as 1). (**C**) moDCs (*upper* and *lower left*) and RA-DCs (*upper* and *lower right*) were immunostained for surface MAdCAM-1 (green) or the IgG control (*lower left*). DAPI-stained nuclei are in blue. Representative results of 1 of 10 different donors are shown. Original magnifications ×40 (*upper row* and *lower left*) and ×100 (*lower right*). Scale bars, 9.95 μm (original magnification ×40) and 10.02 μm (original magnification ×100).

HIV replication (41–46), we cultured the infected moDC–T cell and RA-DC–T cell mixtures in presence of αRAR or a mock solution. Remarkably, HIV replication was significantly higher in the RA-DC–T cell mixtures in presence of αRAR (Fig. 6A), and it was also higher, but not significantly, in the absence of the αRAR. This indicates that changes induced in the DCs by RA, other than the induction of RA-producing capabilities in the DCs, are responsible for driving HIV replication in the RA-DC–T cell milieu. HIV replication in the cocultures treated with αRAR was lower than in their absence (Supplemental Fig. 4A), and this was most likely due to blocking the effect of serum-derived RA and RA released by the RA-DCs on the T cells. The RA-DC–driven increase in HIV infection in the DC–T cell mixtures was not due to an enhanced ability of RA-DCs to capture the virions (Fig. 6B) nor to increased HIV replication in the RA-DCs (Fig. 6C).

Because RA modulated the expression of specific receptors on the DCs, but not others, we investigated whether any of the changes in the expression of these surface proteins could be correlated with the increase in HIV infection in the RA-DC–T cell cocultures. Among all the receptors impacted by RA, only the increase in the expression of MAdCAM-1 correlated with the increase in HIV replication in the cocultures in the presence of αRAR (Fig. 6D). Interestingly, neither the increased expression of CD103, marker of mucosal DCs, nor of CD54, known to impact the formation of virological synapses, correlated with the increase in HIV infection in the cocultures (Fig. 6D).

To further explore the biology of RA-DC–T cell infection, we investigated whether the HIV-infected RA-DC–T cell cultures released different soluble factors than the infected moDC–T cell cultures. Supernatants from days 3 and 6 of the cocultures were analyzed by 25-Plex luminex, but no significant differences were noted (data not shown). Similar to the RA-DC cultures (Fig. 2), more CCL2 was detected in the RA-DC–T cell mixtures, but the difference was not significant. RA-DC–T cell cocultures released slightly lower amounts of the inflammatory cytokines CXCL-10 (*IP-10*) and IFN-γ, but this was also not significant (data not shown).

Blocking MAdCAM-1 partially decreases the enhanced ability of RA-DCs to fuel HIV infection

Because we determined that the RA-driven increase in MAdCAM-1 expression on RA-DCs correlated with the increase in HIV replication in the RA-DC–T cell cultures, we hypothesized that MAdCAM-1 could be involved, at least partially, in the enhancement of viral replication. First, we investigated whether the presence of the anti–MAdCAM-1 mAb clone 314G8 had an impact on DC–T conjugate formation. We found that blocking MAdCAM-1 did not change the frequency of conjugates, whereas, as previously reported (47), blocking of CD54 reduced conjugate formation of ∼50%. However, this was independent of the DC treatment and of presence of αRAR (Supplemental Fig. 4C). Subsequently, we compared the HIV infection levels in presence or absence of the anti–MAdCAM-1 mAb. When the anti–MAdCAM-1 mAb was added, the increase in

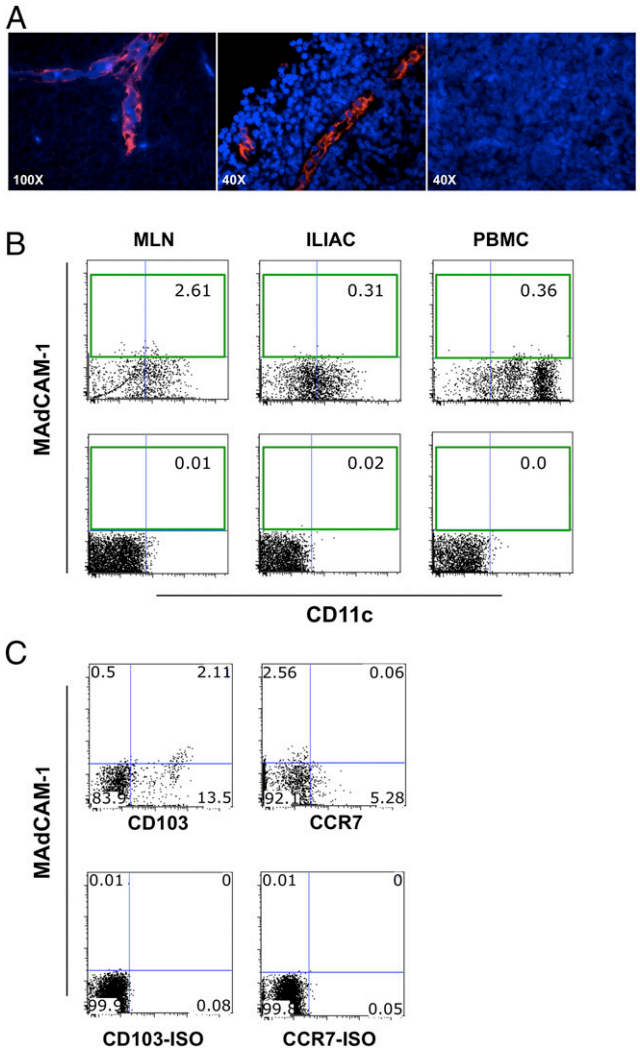

FIGURE 4. MAdCAM-1 on a small population of MLNs DCs. (**A**) MLNs from uninfected healthy rhesus macaques were stained with the anti–MAdCAM-1 mAb clone 314G8 (red; *left* and *center*) or an isotype control (*right*). Nuclei were detected with DAPI (blue). (**B**) A representative plot from MLN, iliac lymph nodes (ILIAC), and blood (PBMC) of 1 of 15 macaques (*upper level*) and isotype control (*lower level*). Cells were gated on live, singlets, Lin^-, and $HLA\text{-}DR^+$. (**C**) Representative plots of Lin^- $HLA\text{-}DR^+$ cells in MLN from the same animal as in (B) showing the $CD103^+$ $CCR7^-$ phenotype of $MAdCAM\text{-}1^+$ DCs.

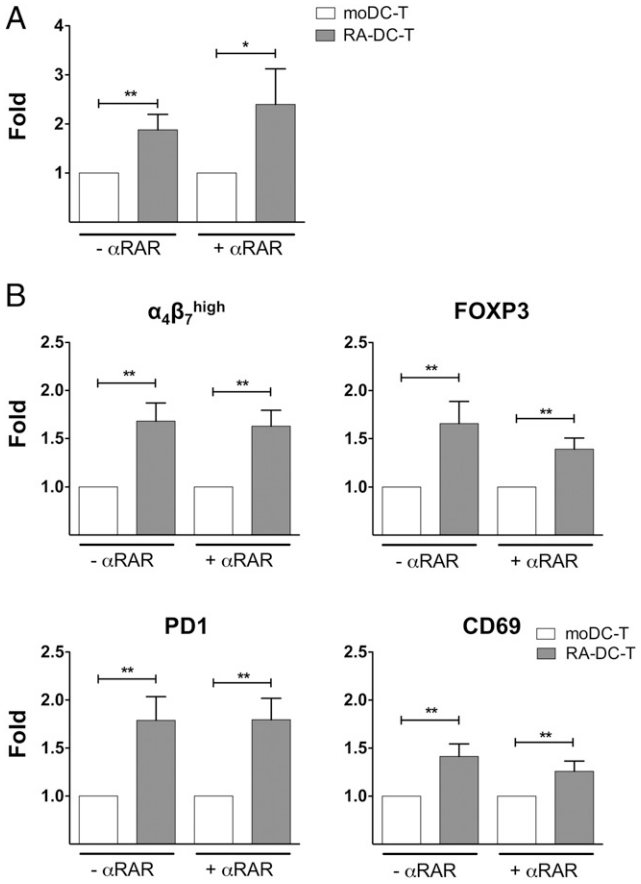

FIGURE 5. \RA treatment of moDCs increases DC–T cell conjugate formation and induces a T regulatory phenotype. (**A**) The fold increase (mean ± SEM, $n = 9$) in the frequency of DC–T cell conjugates (percentage of events positive for CD3 staining within the large DC gate) in RA-DC–T cell cocultures in the absence and in presence of αRAR compared with moDC–T cell cocultures (set as 1) is shown. (**B**) The fold increase (mean ± SEM, $n = 9$) in the frequency of $\alpha_4\beta_7^{high}$, $FOXP3^+$, $PD1^+$, and $CD69^+$ $CD4^+$ T cells in RA-DC–T cell versus moDC–T cell mixtures is shown (without or with the addition of αRAR). $^*p < 0.05$ is considered significant, $^{**}p < 0.01$.

HIV infection seen in the RA-DC–T cell cocultures in presence of the αRAR was no longer significant (relative to the respective moDC controls; Fig. 7). In absence of the αRAR, the infection in the RA-DC–T cell mixtures was reduced to the levels seen in the moDC–T cells. No difference in HIV replication was noted between moDC–T cell cocultures in presence or absence of the anti–MAdCAM-1 mAb (Supplemental Fig. 4B).

Discussion

The GALT is a primary site of HIV expansion and dissemination after mucosal exposure, and its disruption correlates with HIV disease progression (11, 13, 48). Moreover, loss of $CD103^+$ mucosal DCs has been associated with damage in the gut tissue (49). Hence, DCs in this anatomical location play a decisive role in HIV transmission and pathogenesis. However, how the intestinal environment shapes the ability of DCs to fuel HIV infection has never been investigated. DCs in the LP, PPs, and MLNs, but not in the skin or peripheral LNs, have the unique ability to produce RA. Gut DCs gain this hallmark feature during their education and maturation in the intestinal compartment, and RA itself has a key role in shaping the DC phenotype (16, 23, 50, 51).

In this study, we describe in detail the effect of RA on specific markers of DC maturation; on receptors involved in HIV attachment, internalization, and infection; and on adhesion molecules important for DC trafficking. After extensive phenotyping of human RA-DCs, we found that RA conditioning increased the expression of some maturation markers, not affecting or reducing the expression of others such as CD80 and CD206. Thus, RA-DCs appear to have a semimature phenotype. Notably, our results confirm other reports that RA increases the expression of CD103 (36), a marker of mucosal DCs in both mice and humans (50). We also found a substantial increase in the expression of CD141. High levels of this receptor are expressed by cross-presenting human DCs with functional homology to mouse CD103, and LN DCs that express high levels of CD103 coexpress high levels of CD141 (52, 53). Moreover, human gut $CD103^+$ $Sirp\alpha^-$ (human single-positive) DCs share significant similarities with human blood $CD141^+$ DCs (50). Although the monocytic origin of LP $CD103^+$ DCs is disputed (54), CD103 pairing with β_7 forms integrin $\alpha_E\beta_7$, which is essential for cell trafficking and retention within the epithelium of mucosal tissues. Moreover, we found that RA-DCs secrete higher amounts of total TGF-β1, which is an important

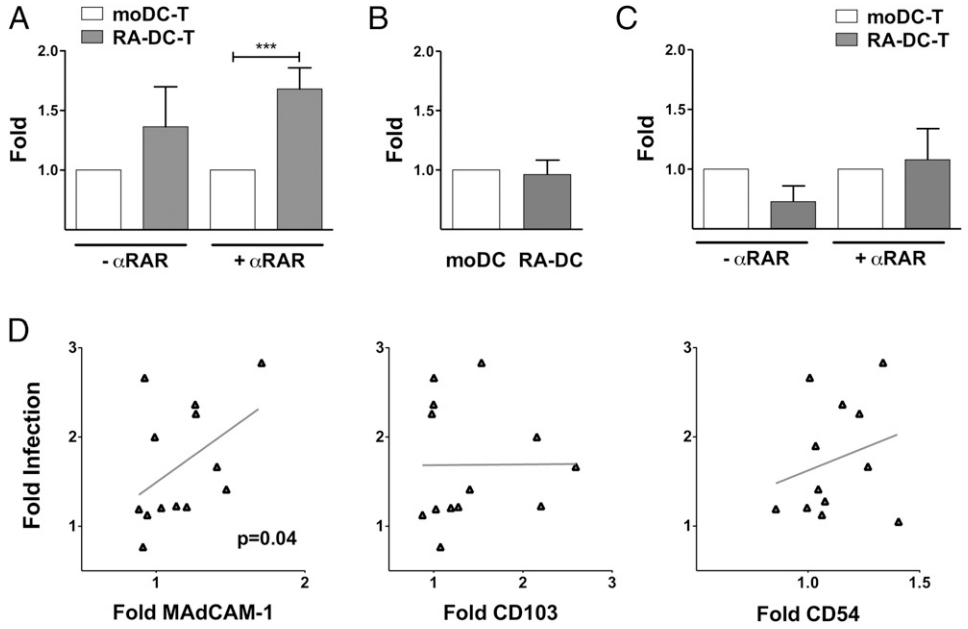

FIGURE 6. RA-DCs drive greater HIV replication than moDCs in DC–T cell cultures. (**A**) The fold increase in HIV copies/cell (mean ± SEM, $n = 7$–10) for the RA-DC–T cell cultures is shown compared with the control moDC–T cell mixtures (set as 1) in the absence and presence of αRAR (***$p < 0.001$). The fold increase in the mean fluorescence intensity of the anti-p24 staining of HIV-pulsed DCs (**B**) and in HIV copies/cell of day 6-infected DC cultures (**C**) (mean ± SEM, $n = 8$) is shown for RA-DCs versus moDCs (set as 1). (**D**) The fold increases in the mean fluorescence intensity of MAdCAM-1, CD54, and CD103 on RA-DCs compared with moDCs (set as 1) are plotted against the fold increases in infection (HIV copies/cell) in the RA-DC–T cell mixtures (over moDC–T cell infections) with αRAR (each dot represents 1 donor run in triplicate; $n = 9$–12). The linear regression fitting line and the Spearman rank correlation p values are shown ($p < 0.05$ is considered significant).

factor in the maintenance of the tolerogenic gut environment. TGF-β1 is critical to the differentiation of iTreg acting in synergy with RA (18). In line with this, we showed that RA-DCs induced the expression of FOXP3, PD1, and CD69 on cocultured T cells, all three important markers of iTreg phenotype (39, 55). This was also true when the T cells were pretreated with αRAR, suggesting that the effect of RA-DCs in T cells is mediated either by TGF-β1 alone or by additional RA-driven changes in DCs. Notably, the increase in the frequency of $\alpha_4\beta_7^{high}$ $CD4^+$ T cells was still present after blocking the ability of $CD4^+$ T cells to respond to RA. The meaning and mechanism of this finding need further investigation. We could not detect the activated form of TGF-β1 in most of the samples probably because the sensitivity of the assay was too low. Nonetheless, an increased amount of total TGF-β1 in the gut microenvironment could be transformed in bioactive TGF-β1 by additional state-specific stimuli. In fact, upon stimulation with anti-CD40 agonist murine bone marrow, RA-DCs were shown to release more bioactive TGF-β1 (21). Our data on FOXP3 expression by $CD4^+$ T cells agree with the murine model of RA-DCs described by Feng et al. (21), but differ from those of Bakdash et al. (36). This may be due to the several differences between our models of human RA-DCs and RA-DC–T cell cultures. The differences include the use in Bakdash et al.'s (36) work of allogeneic naive $CD4^+$ T cells and generation of RA-DCs with the addition of RA from day 0. Moreover, most of their conclusions are drawn by data on LPS-activated RA-DCs. In line with the RA-DCs' mostly tolerogenic phenotype, in our model, RA-DCs released more IL-10, whereas, although significant, the increase in inflammatory cytokines was very small. RA treatment also substantially increased the release of the Th2-skewing chemokine CCL2, suggesting that RA-conditioned DCs may also regulate a Th2 type of response (37).

One of the most intriguing and possibly controversial findings of our work was the detection of MAdCAM-1 on moDCs, which seems to be increased by RA conditioning. In vivo, we detected MAdCAM-1 on the surface of a small population of DCs in rhesus macaque MLNs. Notably, only clones against the Ig domain, but not the mucin domain, recognized MAdCAM-1 on both human and macaque DCs. This may be explained by the existence of alternatively spliced variants that lack either parts of the second Ig domain, or all or part of the mucin domain (56, 57). These findings indicate that the expression of MAdCAM-1 may be highly specific, and its function may be regulated by extensive modifications to its multidomain structure (56). Considering that the primary focus of our work was to investigate the effect of RA on the ability of DCs to spread HIV, a more thorough investigation of the expression of MAdCAM-1 by DCs will be part of future work.

Remarkably, we demonstrated that, compared with immature moDCs, RA-DCs have an enhanced ability to augment HIV infection in DC–T cell cultures. This increase was significant when the RARs

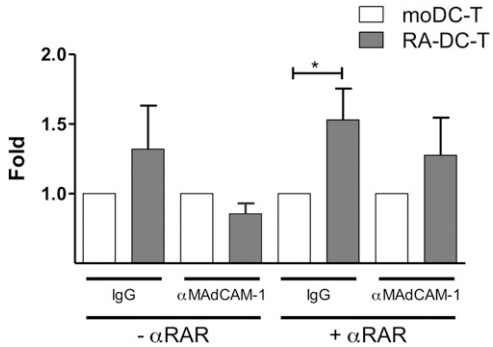

FIGURE 7. Blocking MAdCAM-1 protein reduced RA-DC's enhanced ability to increase HIV infection. DC–T cell cocultures were set up (in the presence or absence of αRAR) with RA-DCs or moDCs pretreated with IgG or anti–MAdCAM-1 (αMAdCAM-1). The fold increases in HIV infection (HIV copies/cell) in RA-DC–T cell versus moDC–T cell cultures (set as 1) are shown (mean ± SEM, $n = 7$). *$p < 0.05$ is considered significant.

were blocked. It is likely that the presence of the antagonists reduced the intra-assay variability due to the effect of serum-derived and DC-derived RA, which can directly modulate $CD4^+$ T cell activation and HIV replication (41–43, 45) and possibly mask the enhancing effect due to RA-DCs. Thus, we found that RA treatment modulates the DC phenotype in a way that increases their ability to fuel HIV replication independent of the presence of RA or other gut-specific factors. Ultimately, the influence of the gut microenvironment on HIV replication will be driven by the sum of the many effects of RA, TGF-β1, and other gut-specific factors and will require further exploration in more complex systems. RA-DCs expressed significantly more CD4, CCR5, and CXCR4; they were not more susceptible to HIV infection; and they did not have an increased ability to capture/internalize the virus. In contrast, the higher frequency of DC–T cell conjugates, as well as an increased availability of highly susceptible $\alpha_4\beta_7^{high}$ $CD4^+$ T cells, may play a role in the enhanced HIV replication in the RA-DC–T cell cocultures by increasing the efficiency of viral transfer from DCs to T cells. Although the RA-driven increase in MAdCAM-1 expression on DCs suggests a role for MAdCAM-1 in the RA-DC–mediated increase in HIV replication, blocking this receptor only partially reduced the infection in the RA-DC–T cell cocultures and had little effect on the moDC–T cell mixtures. Thus, MAdCAM-1–increased expression alone does not explain the RA-DC–driven increase in HIV replication. Nonetheless, enhanced MAdCAM-1 interaction with $\alpha_4\beta_7$ on the $CD4^+$ T cells may induce a stronger costimulatory signal, increasing cell activation and HIV replication (58). This could explain why blocking MAdCAM-1 reduced the RA-DC–driven enhancement of HIV replication, while having no effect on conjugate formation. The αMAdCAM-1 inhibitory effect appears stronger in absence of αRAR. This might be due to the fact that the initial increase in HIV replication was lower (nonsignificant) or a specific effect created by blocking MAdCAM-1 in presence of RA.

Finally, we found that RA increases the expression of CD54, but this did not correlate with the increase in HIV replication, and that blocking CD54 inhibited DC–T cell conjugate formation, but this was independent of RA treatment of DCs. Blockage of CD54 would disrupt HIV transfer between DCs and $CD4^+$ T cells independent of RA treatment of DCs and cannot explain the increase in HIV replication specifically due to RA treatment of DCs. Other not yet identified DC receptors could be influenced by RA treatment and play a role in the RA-DCs' increased ability to drive HIV infection.

In conclusion, in this work, we describe the effect of RA, a key mediator of the intestinal immunological response, on an array of DC surface receptors and soluble factors. To our knowledge, we report for the first time the detection of MAdCAM-1 on DCs and its increase by RA treatment. Our results suggest that in a RA-rich microenvironment, such as the small intestine and the GALT, DCs interact with $CD4^+$ T cells in a way that supports higher levels of HIV replication. Considering the importance of the GALT in HIV transmission, pathogenesis, and establishment and maintenance of the HIV reservoir (12, 13), our results suggest that the mechanisms of HIV expansion in this anatomical site may be different from those known in blood, genital submucosa, and skin. An increased awareness of these mechanisms is key to the development of effective means of HIV eradication.

Acknowledgments

We thank Drs. Jeffrey Lifson and Julian Bess for providing the HIV-BaL used for this study, the staff of the Population Council Cell Biology and Flow Cytometry Facility, and the staff of TNPRC for continued support.

Disclosures

The authors have no financial conflicts of interest.

References

1. Pope, M., M. G. H. Betjes, N. Romani, H. Hirmand, P. U. Cameron, L. Hoffman, S. Gezelter, G. Schuler, and R. M. Steinman. 1994. Conjugates of dendritic cells and memory T lymphocytes from skin facilitate productive infection with HIV-1. *Cell* 78: 389–398.
2. Derby, N., E. Martinelli, and M. Robbiani. 2011. Myeloid dendritic cells in HIV-1 infection. *Curr. Opin. HIV AIDS* 6: 379–384.
3. Peressin, M., A. Proust, S. Schmidt, B. Su, M. Lambotin, M. E. Biedma, G. Laumond, T. Decoville, V. Holl, and C. Moog. 2014. Efficient transfer of HIV-1 in trans and in cis from Langerhans dendritic cells and macrophages to autologous T lymphocytes. *AIDS* 28: 667–677.
4. Turville, S. G., M. Aravantinou, H. Stössel, N. Romani, and M. Robbiani. 2008. Resolution of de novo HIV production and trafficking in immature dendritic cells. *Nat. Methods* 5: 75–85.
5. McDonald, D. 2010. Dendritic cells and HIV-1 trans-infection. *Viruses* 2: 1704–1717.
6. Rinaldo, C. R. 2013. HIV-1 trans infection of CD4(+) T cells by professional antigen presenting cells. *Scientifica* 2013: 164203.
7. Wilkinson, J., and A. L. Cunningham. 2006. Mucosal transmission of HIV-1: first stop dendritic cells. *Curr. Drug Targets* 7: 1563–1569.
8. Harman, A. N., M. Kim, N. Nasr, K. J. Sandgren, and P. U. Cameron. 2013. Tissue dendritic cells as portals for HIV entry. *Rev. Med. Virol.* 23: 319–333.
9. Boltjes, A., and F. van Wijk. 2014. Human dendritic cell functional specialization in steady-state and inflammation. *Front. Immunol.* 5: 131.
10. Veazey, R. S., M. DeMaria, L. V. Chalifoux, D. E. Shvetz, D. R. Pauley, H. L. Knight, M. Rosenzweig, R. P. Johnson, R. C. Desrosiers, and A. A. Lackner. 1998. Gastrointestinal tract as a major site of CD4+ T cell depletion and viral replication in SIV infection. *Science* 280: 427–431.
11. Mehandru, S., M. A. Poles, K. Tenner-Racz, A. Horowitz, A. Hurley, C. Hogan, D. Boden, P. Racz, and M. Markowitz. 2004. Primary HIV-1 infection is associated with preferential depletion of CD4+ T lymphocytes from effector sites in the gastrointestinal tract. *J. Exp. Med.* 200: 761–770.
12. Mattapallil, J. J., D. C. Douek, B. Hill, Y. Nishimura, M. Martin, and M. Roederer. 2005. Massive infection and loss of memory CD4+ T cells in multiple tissues during acute SIV infection. *Nature* 434: 1093–1097.
13. Mehandru, S., M. A. Poles, K. Tenner-Racz, V. Manuelli, P. Jean-Pierre, P. Lopez, A. Shet, A. Low, H. Mohri, D. Boden, et al. 2007. Mechanisms of gastrointestinal CD4+ T-cell depletion during acute and early human immunodeficiency virus type 1 infection. *J. Virol.* 81: 599–612.
14. Brenchley, J. M., and D. C. Douek. 2008. HIV infection and the gastrointestinal immune system. *Mucosal Immunol.* 1: 23–30.
15. Haase, A. T. 2005. Perils at mucosal front lines for HIV and SIV and their hosts. *Nat. Rev. Immunol.* 5: 783–792.
16. Scott, C. L., A. M. Aumeunier, and A. M. Mowat. 2011. Intestinal CD103+ dendritic cells: master regulators of tolerance? *Trends Immunol.* 32: 412–419.
17. Jaensson, E., H. Uronen-Hansson, O. Pabst, B. Eksteen, J. Tian, J. L. Coombes, P. L. Berg, T. Davidsson, F. Powrie, B. Johansson-Lindbom, and W. W. Agace. 2008. Small intestinal CD103+ dendritic cells display unique functional properties that are conserved between mice and humans. *J. Exp. Med.* 205: 2139–2149.
18. Mucida, D., K. Pino-Lagos, G. Kim, E. Nowak, M. J. Benson, M. Kronenberg, R. J. Noelle, and H. Cheroutre. 2009. Retinoic acid can directly promote TGF-beta-mediated Foxp3(+) Treg cell conversion of naive T cells. *Immunity* 30: 471–472, author reply 472–473.
19. Mora, J. R., M. Iwata, and U. H. von Andrian. 2008. Vitamin effects on the immune system: vitamins A and D take centre stage. *Nat. Rev. Immunol.* 8: 685–698.
20. Cassani, B., E. J. Villablanca, J. De Calisto, S. Wang, and J. R. Mora. 2012. Vitamin A and immune regulation: role of retinoic acid in gut-associated dendritic cell education, immune protection and tolerance. *Mol. Aspects Med.* 33: 63–76.
21. Feng, T., Y. Cong, H. Qin, E. N. Benveniste, and C. O. Elson. 2010. Generation of mucosal dendritic cells from bone marrow reveals a critical role of retinoic acid. *J. Immunol.* 185: 5915–5925.
22. Iliev, I. D., E. Mileti, G. Matteoli, M. Chieppa, and M. Rescigno. 2009. Intestinal epithelial cells promote colitis-protective regulatory T-cell differentiation through dendritic cell conditioning. *Mucosal Immunol.* 2: 340–350.
23. Vicente-Suarez, I., A. Larange, C. Reardon, M. Matho, S. Feau, G. Chodaczek, Y. Park, Y. Obata, R. Gold, Y. Wang-Zhu, et al. 2015. Unique lamina propria stromal cells imprint the functional phenotype of mucosal dendritic cells. *Mucosal Immunol.* 8: 141–151.
24. Klebanoff, C. A., S. P. Spencer, P. Torabi-Parizi, J. R. Grainger, R. Roychoudhuri, Y. Ji, M. Sukumar, P. Muranski, C. D. Scott, J. A. Hall, et al. 2013. Retinoic acid controls the homeostasis of pre-cDC-derived splenic and intestinal dendritic cells. *J. Exp. Med.* 210: 1961–1976.
25. Tao, Y., Y. Yang, and W. Wang. 2006. Effect of all-trans-retinoic acid on the differentiation, maturation and functions of dendritic cells derived from cord blood monocytes. *FEMS Immunol. Med. Microbiol.* 47: 444–450.
26. Iwata, M., A. Hirakiyama, Y. Eshima, H. Kagechika, C. Kato, and S. Y. Song. 2004. Retinoic acid imprints gut-homing specificity on T cells. *Immunity* 21: 527–538.
27. Cicala, C., E. Martinelli, J. P. McNally, D. J. Goode, R. Gopaul, J. Hiatt, K. Jelicic, S. Kottilil, K. Macleod, A. O'Shea, et al. 2009. The integrin alpha4beta7 forms a complex with cell-surface CD4 and defines a T-cell subset that is highly susceptible to infection by HIV-1. *Proc. Natl. Acad. Sci. USA* 106: 20877–20882.
28. Kader, M., S. Bixler, M. Roederer, R. Veazey, and J. J. Mattapallil. 2009. CD4 T cell subsets in the mucosa are CD28+Ki-67-HLA-DR-CD69+ but show dif-

ferential infection based on alpha4beta7 receptor expression during acute SIV infection. *J. Med. Primatol.* 38(Suppl. 1): 24–31.
29. Martinelli, E., F. Veglia, D. Goode, N. Guerra-Perez, M. Aravantinou, J. Arthos, M. Piatak, Jr., J. D. Lifson, J. Blanchard, A. Gettie, and M. Robbiani. 2013. The frequency of alpha4beta7high memory CD4+ T cells correlates with susceptibility to rectal SIV infection. J. Acquir. Immune Defic. Syndr. *64: 325-331.*
30. Byrareddy, S. N., B. Kallam, J. Arthos, C. Cicala, F. Nawaz, J. Hiatt, E. N. Kersh, J. M. McNicholl, D. Hanson, K. A. Reimann, et al. 2014. Targeting α4β7 integrin reduces mucosal transmission of simian immunodeficiency virus and protects gut-associated lymphoid tissue from infection. *Nat. Med.* 20: 1397–1400.
31. Kobayashi, M., H. Hoshino, K. Suzawa, Y. Sakai, J. Nakayama, and M. Fukuda. 2012. Two distinct lymphocyte homing systems involved in the pathogenesis of chronic inflammatory gastrointestinal diseases. *Semin. Immunopathol.* 34: 401–413.
32. Leung, E., R. K. Kanwar, J. R. Kanwar, and G. W. Krissansen. 2003. Mucosal vascular addressin cell adhesion molecule-1 is expressed outside the endothelial lineage on fibroblasts and melanoma cells. *Immunol. Cell Biol.* 81: 320–327.
33. Douek, D. C., J. M. Brenchley, M. R. Betts, D. R. Ambrozak, B. J. Hill, Y. Okamoto, J. P. Casazza, J. Kuruppu, K. Kunstman, S. Wolinsky, et al. 2002. HIV preferentially infects HIV-specific CD4+ T cells. *Nature* 417: 95–98.
34. Johansson-Lindbom, B., M. Svensson, O. Pabst, C. Palmqvist, G. Marquez, R. Förster, and W. W. Agace. 2005. Functional specialization of gut CD103+ dendritic cells in the regulation of tissue-selective T cell homing. *J. Exp. Med.* 202: 1063–1073.
35. Springer, T. A., and M. L. Dustin. 2012. Integrin inside-out signaling and the immunological synapse. *Curr. Opin. Cell Biol.* 24: 107–115.
36. Bakdash, G., L. T. Vogelpoel, T. M. van Capel, M. L. Kapsenberg, and E. C. de Jong. 2014. Retinoic acid primes human dendritic cells to induce gut-homing, IL-10-producing regulatory T cells. *Mucosal Immunol*. DOI: 10.1038/mi.2014.64.
37. Gu, L., S. Tseng, R. M. Horner, C. Tam, M. Loda, and B. J. Rollins. 2000. Control of TH2 polarization by the chemokine monocyte chemoattractant protein-1. *Nature* 404: 407–411.
38. Szabo, M. C., E. C. Butcher, and L. M. McEvoy. 1997. Specialization of mucosal follicular dendritic cells revealed by mucosal addressin-cell adhesion molecule-1 display. *J. Immunol*. 158: 5584–5588.
39. Cortés, J. R., R. Sánchez-Díaz, E. R. Bovolenta, O. Barreiro, S. Lasarte, A. Matesanz-Marín, M. L. Toribio, F. Sánchez-Madrid, and P. Martín. 2014. Maintenance of immune tolerance by Foxp3(+) regulatory T cells requires CD69 expression. *J. Autoimmun.* 55: 51–62.
40. Amarnath, S., C. W. Mangus, J. C. Wang, F. Wei, A. He, V. Kapoor, J. E. Foley, P. R. Massey, T. C. Felizardo, J. L. Riley, et al. 2011. The PDL1-PD1 axis converts human TH1 cells into regulatory T cells. *Sci. Transl. Med.* 3: ra120.
41. Hall, J. A., J. L. Cannons, J. R. Grainger, L. M. Dos Santos, T. W. Hand, S. Naik, E. A. Wohlfert, D. B. Chou, G. Oldenhove, M. Robinson, et al. 2011. Essential role for retinoic acid in the promotion of CD4(+) T cell effector responses via retinoic acid receptor alpha. *Immunity* 34: 435–447.
42. Bidad, K., E. Salehi, M. Oraei, A. A. Saboor-Yaraghi, and M. H. Nicknam. 2011. Effect of all-trans retinoic acid (ATRA) on viability, proliferation, activation and lineage-specific transcription factors of CD4+ T cells. *Iran. J. Allergy Asthma Immunol.* 10: 243–249.
43. Turpin, J. A., M. Vargo, and M. S. Meltzer. 1992. Enhanced HIV-1 replication in retinoid-treated monocytes: retinoid effects mediated through mechanisms related to cell differentiation and to a direct transcriptional action on viral gene expression. *J. Immunol.* 148: 2539–2546.
44. Yamaguchi, K., J. E. Groopman, and R. A. Byrn. 1994. The regulation of HIV by retinoic acid correlates with cellular expression of the retinoic acid receptors. *AIDS* 8: 1675–1682.
45. Towers, G., J. Harris, G. Lang, M. K. Collins, and D. S. Latchman. 1995. Retinoic acid inhibits both the basal activity and phorbol ester-mediated activation of the HIV long terminal repeat promoter. *AIDS* 9: 129–136.
46. Zoumpourlis, V., M. Ergazaki, and D. A. Spandidos. 1996. Transcriptional activation of the human immunodeficiency virus long terminal repeat sequences by retinoic acid in human epithelial and fibroblast tumor cell lines. *Int. J. Biol. Markers* 11: 153–158.
47. Rodriguez-Plata, M. T., I. Puigdomènech, N. Izquierdo-Useros, M. C. Puertas, J. Carrillo, I. Erkizia, B. Clotet, J. Blanco, and J. Martinez-Picado. 2013. The infectious synapse formed between mature dendritic cells and CD4(+) T cells is independent of the presence of the HIV-1 envelope glycoprotein. *Retrovirology* 10: 42.
48. Hofer, U., and R. F. Speck. 2009. Disturbance of the gut-associated lymphoid tissue is associated with disease progression in chronic HIV infection. *Semin. Immunopathol.* 31: 257–266.
49. Klatt, N. R., J. D. Estes, X. Sun, A. M. Ortiz, J. S. Barber, L. D. Harris, B. Cervasi, L. K. Yokomizo, L. Pan, C. L. Vinton, et al. 2012. Loss of mucosal CD103+ DCs and IL-17+ and IL-22+ lymphocytes is associated with mucosal damage in SIV infection. *Mucosal Immunol.* 5: 646–657.
50. Watchmaker, P. B., K. Lahl, M. Lee, D. Baumjohann, J. Morton, S. J. Kim, R. Zeng, A. Dent, K. M. Ansel, B. Diamond, et al. 2014. Comparative transcriptional and functional profiling defines conserved programs of intestinal DC differentiation in humans and mice. *Nat. Immunol.* 15: 98–108.
51. Iliev, I. D., I. Spadoni, E. Mileti, G. Matteoli, A. Sonzogni, G. M. Sampietro, D. Foschi, F. Caprioli, G. Viale, and M. Rescigno. 2009. Human intestinal epithelial cells promote the differentiation of tolerogenic dendritic cells. *Gut* 58: 1481–1489.
52. Haniffa, M., A. Shin, V. Bigley, N. McGovern, P. Teo, P. See, P. S. Wasan, X. N. Wang, F. Malinarich, B. Malleret, et al. 2012. Human tissues contain CD141hi cross-presenting dendritic cells with functional homology to mouse CD103+ nonlymphoid dendritic cells. *Immunity* 37: 60–73.
53. van de Ven, R., M. F. van den Hout, J. J. Lindenberg, B. J. Sluijter, P. A. van Leeuwen, S. M. Lougheed, S. Meijer, M. P. van den Tol, R. J. Scheper, and T. D. de Gruijl. 2011. Characterization of four conventional dendritic cell subsets in human skin-draining lymph nodes in relation to T-cell activation. *Blood* 118: 2502–2510.
54. Bogunovic, M., F. Ginhoux, J. Helft, L. Shang, D. Hashimoto, M. Greter, K. Liu, C. Jakubzick, M. A. Ingersoll, M. Leboeuf, et al. 2009. Origin of the lamina propria dendritic cell network. *Immunity* 31: 513–525.
55. Gianchecchi, E., D. V. Delfino, and A. Fierabracci. 2013. Recent insights into the role of the PD-1/PD-L1 pathway in immunological tolerance and autoimmunity. *Autoimmun. Rev.* 12: 1091–1100.
56. Leung, E., J. Greene, J. Ni, L. G. Raymond, K. Lehnert, R. Langley, and G. W. Krissansen. 1996. Cloning of the mucosal addressin MAdCAM-1 from human brain: identification of novel alternatively spliced transcripts. *Immunol. Cell Biol.* 74: 490–496.
57. Sampaio, S. O., X. Li, M. Takeuchi, C. Mei, U. Francke, E. C. Butcher, and M. J. Briskin. 1995. Organization, regulatory sequences, and alternatively spliced transcripts of the mucosal addressin cell adhesion molecule-1 (MAdCAM-1) gene. *J. Immunol.* 155: 2477–2486.
58. Teague, T. K., A. I. Lazarovits, and B. W. McIntyre. 1994. Integrin alpha 4 beta 7 co-stimulation of human peripheral blood T cell proliferation. *Cell Adhes. Commun.* 2: 539–547.